Journal of Sound and Vibration (1997) **208**(3), 427–439

STABILITY AND CHAOTIC MOTIONS OF A RESTRAINED PIPE CONVEYING FLUID

J.-D. JIN

Department of Aeronautical Engineering, Shenyang Institute of Aeronautical Engineering, Shenyang 110034, *People's Republic of China*

(*Received* 13 *September* 1996, *and in final form* 18 *June* 1997)

The stability and dynamics of a cantilevered pipe conveying fluid with motion-limiting constraints and an elastic support have been investigated. Attention was concentrated on the behaviour of the system in the region of dynamic instability, and several motions were found by using the method of numerical simulations. The effect of the spring constant and some other parameters on the dynamics of the system was also investigated. It is shown that chaotic motions can occur in this system in a certain region of parameter space.

1. INTRODUCTION

The dynamics of cantilevered pipes conveying fluid has been studied quite extensively by many investigators [1]. Most of the early theoretical work on this problem has been carried out within the framework of linear theory. With the recent developments of the theory on non-linear dynamical systems and chaos, much attention has been paid to the study of possible existence of chaotic motions in some modified systems with strong non-linearities. Tang and Dowell [2] have disclosed the chaotic behaviour of a cantilevered pipe conveying fluid when two permanent magnets are placed to the right and left of the free end of the pipe. Païdoussis and Moon [3] studied, both experimentally and theoretically, the dynamics of a cantilevered pipe which is constrained by non-linear motion restraints. In a range of values of flow velocity beyond the Hopf bifurcation, they found that chaotic motions arise in this autonomous system through a series of period doubling bifurcations. A series of studies on this topic was done by Païdoussis *et al*. [3–6] to complete their work from various aspects. More recently, Li and Païdoussis [7] studied certain non-linear equations of motion of a "standing" cantilevered pipe conveying fluid by using the perturbation technique and Galerkin's method. They analyzed a doubly degenerate case in which the system possesses a zero eigenvalue and a pair of purely imaginary eigenvalues. The theory of the centre manifold and normal forms and the Melnikov method were applied in the analysis to obtain the local codimension two unfolding as well as to provide possible parameter regions in which chaotic motions may arise.

In this paper the planar dynamics of a cantilevered pipe conveying fluid, as shown in Figure 1, are analyzed. The pipe is restrained by the motion-limiting constraints, and a linear spring support is attached to it at the restrained point. It should be noted that the system without the linear spring support is the same as studied by Païdoussis and Moon [3]. The purpose of the present paper is to investigate the effect of the spring constant and some other parameters on the dynamics of the system. Attention is concentrated on the possible chaotic behaviour of the system which has been shown to occur in the case of

0022–460X/97/480427 + 13 $25.00/0/sv971195

no spring support [3]. It should also be noted that the present model will become the one studied by Sugiyama *et al*. [9] when the motion-limiting constraints are removed.

2. DIFFERENTIAL EQUATION OF MOTION

The system considered is shown in Figure 1. The cantilevered pipe conveying fluid is hanging vertically and subject to planar motions: $y(x, t)$. The pipe axis in its undeformed state coincides with the x-axis, which is in the direction of gravity. In the (x, y) plane, there are motion constraints, positioned with a certain lateral clearance to the pipe and the linear spring support. For details about the mechanical model of the pipe and the motion constraints, the reader should refer to references [3, 8]. Some main assumptions for the system are:

(1) The material of the pipe is viscoelastic and of the Kelvin–Voigt type [8] with viscoelastic coefficient a.

(2) The fluid flow is incompressible and steady with mean velocity U.

(3) The effect of external damping is small and is neglected here.

(4) The effect of the motion constraints and the spring support can be written as the restraining force [3]:

$$f = (K_1 y + K_2 y^3)\,\delta(x - x_b) \tag{1}$$

where δ is the Dirac delta function; K_1 is the stiffness of the spring of the elastic support; K_2 is the stiffness of the cubic spring which represents the effect of the motion constraints. Then, the equation of motion of the pipe may be written as

$$\begin{aligned} aEI\frac{\partial^5 y}{\partial x^4\,\partial t} + EI\frac{\partial^4 y}{\partial x^4} + [MU^2 - (M+m)(L-x)g]\frac{\partial^2 y}{\partial x^2} \\ + (M+m)g\frac{\partial y}{\partial x} + 2MU\frac{\partial^2 y}{\partial x\,\partial t} + (M+m)\frac{\partial^2 y}{\partial t^2} \\ + (K_1 y + K_2 y^3)\,\delta(x - x_b) = 0. \end{aligned} \tag{2}$$

where EI is the flexural rigidity of the pipe, L its length and m its mass per unit length; M is the mass of the fluid per unit length, $y(x, t)$ the lateral deflection of the pipe and g the acceleration due to gravity.

Introducing the following non-dimensional variables and parameters

$$\begin{gathered} \eta = y/L, \quad \xi = x/L, \quad \tau = (EI/[M+m])^{1/2}t/L^2, \quad u = (M/EI)^{1/2}UL, \\ \beta = M/(M+m), \quad \gamma = (M+m)gL^3/EI, \quad k_1 = K_1L^3/EI, \quad k_2 = K_2L^5/EI, \\ \xi_b = x_b/L, \quad \alpha = (EI/[M+m])^{1/2}a/L^2, \end{gathered} \tag{3}$$

equation (2) may be written as a dimensionless form

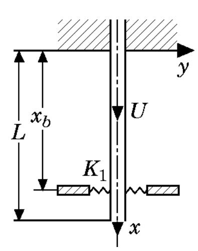

Figure 1. Schematic of the system treated in this paper.

$$\alpha \frac{\partial^5 \eta}{\partial \xi^4 \partial \tau} + \frac{\partial^4 \eta}{\partial \xi^4} + [u^2 - \gamma(1-\xi)] \frac{\partial^2 \eta}{\partial \xi^2} + 2\sqrt{\beta} u \frac{\partial^2 \eta}{\partial \xi \, \partial \tau} + \gamma \frac{\partial \eta}{\partial \xi} + (k_1 \eta + k_2 \eta^3) \, \delta(\xi - \xi_b) + \frac{\partial^2 \eta}{\partial \tau^2} = 0. \tag{4}$$

To discretize equation (4) in accordance with Galerkin's method, let

$$\eta(\xi, \tau) = \sum_{r=1}^{N} \varphi_r(\xi) q_r(\tau), \tag{5}$$

where

$$\varphi_r(\xi) = \cosh \lambda_r \xi - \cos \lambda_r \xi - \sigma_r (\sinh \lambda_r \xi - \sin \lambda_r \xi),$$
$$\sigma_r = [\sinh \lambda_r - \sin \lambda_r]/[\cosh \lambda_r + \cos \lambda_r], \qquad (r = 1, 2, \ldots, N) \tag{6}$$

are the eigenfunctions of the cantilever beam. The dynamics in the lower four-dimensional (two-degree-of-freedom, i.e., $N = 2$) versions of the analytical model in the case of no spring support was found to be in good qualitative agreement, and in good quantitative agreement in some aspects, with experimental observations [3, 5]. For the analytical model ($f(y) = K_2 y^3$) of the restraining force, the convergence of the analytical results was also demonstrated with an increasing number of degrees of freedom (N), in terms of the thresholds of various bifurcations [4, 5]. Since the main purpose of this paper is to investigate part of the qualitative behaviour of the present system, the two-mode expansion ($N = 2$) in equation (5) is adopted in the analytical model for simplicity. Substituting equation (5) into equation (4), employing the orthogonality of the modes [8] and discretization, one can reduce the partial differential equation (4) after laborious calculation to a four-dimensional first order ordinary differential equation:

$$\dot{\mathbf{X}} = \mathbf{AX} + \mathbf{F}(\mathbf{X}), \tag{7}$$

where

$$\mathbf{X} = (x_1, x_2, x_3, x_4)^{\mathrm{T}}, \qquad x_1 = q_1, \qquad x_2 = q_2, \qquad x_3 = \dot{q}_1, \qquad x_4 = \dot{q}_2,$$

$$\mathbf{A} = \begin{bmatrix} 0 & 0 & 1 & 0 \\ 0 & 0 & 0 & 1 \\ a_1 & a_2 & a_3 & a_4 \\ b_1 & b_2 & b_3 & b_4 \end{bmatrix}, \qquad \mathbf{F}(\mathbf{X}) = (0, 0, F_3, F_4)^{\mathrm{T}}$$

$$a_1 = -(\lambda_1^4 + u^2 c_{11} + \gamma e_{11} + k_1 g_{11}), \qquad a_2 = -(u^2 c_{12} + \gamma e_{12} + k_1 g_{12}),$$
$$a_3 = -(\alpha \lambda_1^4 + 2\sqrt{\beta} u b_{11}), \qquad a_4 = -2\sqrt{\beta} u b_{12}, \qquad b_1 = -(u^2 c_{21} + \gamma e_{21} + k_1 g_{21}),$$
$$b_2 = -(\lambda_2^4 + u^2 c_{22} + \gamma e_{22} + k_1 g_{22}), \qquad b_3 = -2\sqrt{\beta} u b_{21}, \qquad b_4 = -(\alpha \lambda_2^4 + 2\sqrt{\beta} u b_{22}),$$
$$F_3 = -k_2 \varphi_1(\xi_b) [\varphi_1(\xi_b) x_1 + \varphi_2(\xi_b) x_2]^3, \qquad F_4 = \varphi_2(\xi_b) F_3 / \varphi_1(\xi_b) = F_3 / e,$$
$$e = \varphi_1(\xi_b)/\varphi_2(\xi_b),$$

$$b_{sr} = \begin{cases} 4/[(\lambda_s/\lambda_r)^2 + (-1)^{r+s}], & r \neq s, \\ 2, & r = s, \end{cases}$$

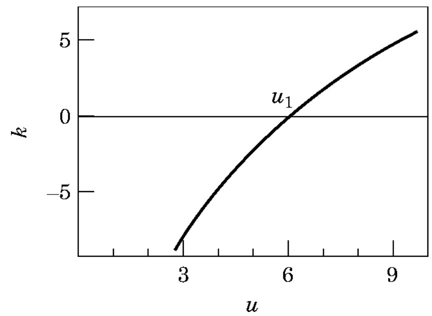

Figure 2. k versus u curve.

$$c_{sr} = \begin{cases} 4(\lambda_r \sigma_r - \lambda_s \sigma_s)/[(-1)^{r+s} - (\lambda_s/\lambda_r)^2], & r \neq s \\ \lambda_r \sigma_r (2 - \lambda_r \sigma_r), & r = s \end{cases}$$

$$d_{sr} = \begin{cases} (-1)^{r+s} 4(\lambda_r \sigma_r - \lambda_s \sigma_s + 2)/[1 - (\lambda_s/\lambda_r)^4] - b_{sr}\,[3 + (\lambda_s/\lambda_r)^4]/[1 - (\lambda_s/\lambda_r)^4], & r \neq s, \\ c_{rr}/2, & r = s, \end{cases}$$

$$e_{sr} = b_{sr} + d_{sr} - c_{sr}, \qquad g_{sr} = \begin{cases} \varphi_s(\xi_b)\varphi_r(\xi_b), & r \neq s, \\ \varphi_r^2(\xi_b), & r = s, \end{cases} \qquad (r = 1, 2);(s = 1, 2), \tag{8}$$

and λ_r $(r = 1, 2)$ represents the eigenvalues of the cantilever beam.

In the next section, one first determines the fixed points of equation (7) which represent the configuration of static deformation of the pipe (equilibria), and then analyze and discuss their stability, mainly in a parameter plane. This information will contribute to the determination of flow behaviour of the system in phase space.

3. STATIC EQUILIBRIA

The equilibria are given by equations

$$a_1 x_1 + a_2 x_2 + F_3 = 0, \qquad b_1 x_1 + b_2 x_2 + F_4 = 0, \qquad x_3 = 0, \qquad x_4 = 0. \tag{9}$$

It is clear that there is always a solution (0, 0, 0, 0) to equations (9), i.e., the origin of X is always a point of equilibrium of the system. Next, one determines the non-zero equilibria of equations (9). Clearly, the non-zero equilibria lie in the (x_1, x_2) plane and are given by the first two equations in equations (9). Since there is the relation, $F_3(X) = eF_4(X)$, between the non-linear terms in equations (9), one can eliminate F_3 and F_4 from equations (9), and obtain

$$x_1 = kx_2, \tag{10}$$

where

$$k = \frac{a_2 - b_2 e}{b_1 e - a_1} = \frac{e\lambda_2^4 + u^2(ec_{22} - c_{12}) + \gamma(ee_{22} - e_{12})}{\lambda_1^4 + u^2(c_{11} - ec_{21}) + \gamma(e_{11} - ee_{21})}. \tag{11}$$

Note that the coefficient k only depends on the parameters γ, ξ_b and u. In what follows, γ, ξ_s, α and β are chosen to be 10, 0·82, 0·005 and 0·2, respectively, in the analysis and numerical computations. Figure 2 shows the k versus u curve generated by equation (11). One can see from this curve and equations (9) that at $u = u_1 \approx 6{\cdot}02294$, $k = 0$, and so for

$u < u_1 k$ is negative, and the sign of x_1 is opposite to the sign of x_2; for $u > u_1 k$ is positive, and x_1 has the same sign with x_2. Substituting equation (10) into equations (9), the equations may be solved to give

$$x_2 = \pm[(a_1 k + a_2)/b]^{1/2}. \tag{12}$$

and one obtains the following three equilibria of the system

$$(1)\ (0, 0, 0, 0) \equiv \{\mathbf{0}\}; \qquad (2)\ (k\sqrt{c}, \sqrt{c}, 0, 0) \equiv +\{\mathbf{N}\};$$
$$(3)\ (-k\sqrt{c}, -\sqrt{c}, 0, 0) \equiv -\{\mathbf{N}\}, \tag{13}$$

where

$$c = (a_1 k + a_2)/b, \qquad b = k_2 g_{11}^2 (k + g_{12}/g_{11})^3. \tag{14}$$

The region where the non-zero equilibria exist is given by the inequality

$$(a_1 k + a_2)/b = e(a_2 b_1 - a_1 b_2)/b(b_1 e - a_1) > 0. \tag{15}$$

Note that

$$e = \varphi_1(\xi_b)/\varphi_2(\xi_b) \approx -4{\cdot}793 < 0,$$
$$b_1 e - a_1 = u^2(c_{11} - c_{21} e) + \gamma(e_{11} - e_{21} e) + \lambda_1^4 > 0, \tag{16}$$

and the sign of b is the same as the sign of $(k + g_{12}/g_{11})$. Let

$$k_0 \equiv -g_{12}/g_{11} = -1/e \approx 0{\cdot}2086336 \tag{17}$$

Substituting $k = k_0$ into equation (11), one obtains the corresponding value of u:

$$u \approx 6{\cdot}10935 \equiv u_0 \tag{18}$$

Then, b is negative when $k < k_0$ (or $u < u_0$), and positive when $k > k_0$ (or $u > u_0$). In the light of the above discussion, one concludes from inequality (15) that the region where the non-zero equilibria exist is given by

$$a_2 b_1 - a_1 b_2 > 0, \qquad \text{for} \qquad u < u_0, \tag{19}$$

and

$$a_2 b_1 - a_1 b_2 < 0, \qquad \text{for} \qquad u > u_0. \tag{20}$$

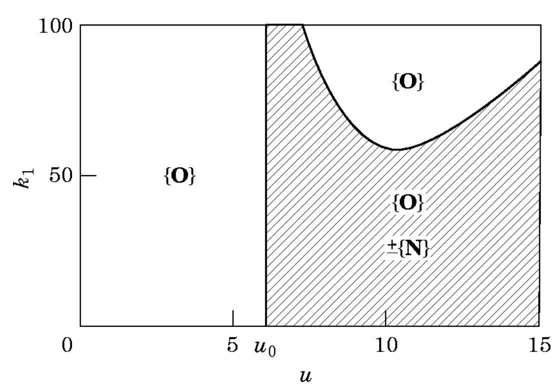

Figure 3. Existence region of non-zero equilibria. The domain marked by diagonal lines indicates the existence of non-zero equilibria.

Because the set of inequalities (19) is empty, the existence domain of the non-zero equilibria is then given only by inequalities (20) and shown in Figure 3.

Note that the co-ordinates x_1 and x_2 of the non-zero equilibria tend to infinity when k tends to k_0 from the right (or, when u tends to u_0 from the right).

4. STABILITY OF EQUILIBRIA

One now analyzes the stability of the equilibrium configuration by considering small disturbances about it. If the disturbances decrease with time then the equilibrium is stable. Mathematically, one can determine the stability according to the linear approximation of the system in the neighbourhood of the equilibrium; that is, the stability of the equilibrium depends on the eigenvalues of the Jacobi matrix, evaluated at the corresponding equilibrium, of the right side in equation (7). For stability all the eigenvalues are negative (or, complex with negative real parts), and for instability at least one of the eigenvalues is positive (or, complex with positive real part). The case with zero (or pure imaginary) eigenvalues constitutes what is referred to as critical behaviour. When the parameters vary and the system passes through the critical state the type of stability of the equilibrium points can change and the number of equilibrium points can change as well. Mathematically, these changes are referred to as bifurcations of solutions.

The Jacobi matrix of the right side in equation (7) has the form

$$\mathbf{J} = \begin{bmatrix} 0 & 0 & 1 & 0 \\ 0 & 0 & 0 & 1 \\ c_1 & c_2 & c_3 & c_4 \\ d_1 & d_2 & d_3 & d_4 \end{bmatrix}, \tag{21}$$

where

$$c_1 = a_1 + \partial F_3/\partial x_1 = a_1 - k_2 g_{11} E(x_1, x_2),$$

$$c_2 = a_2 + \partial F_3/\partial x_2 = a_2 - k_2 g_{12} E(x_1, x_2),$$

$$c_3 = a_3, \qquad c_4 = a_4, \qquad d_1 = b_1 + \partial F_4/\partial x_1 = b_1 - k_2 g_{21} E(x_1, x_2),$$

$$d_2 = b_2 + \partial F_4/\partial x_2 = b_2 - k_2 g_{22} E(x_1, x_2), \qquad d_3 = b_3, \qquad d_4 = b_4,$$

$$E(x_1, x_2) = 3[\varphi_1(\xi_b)x_1 + \varphi_2(\xi_b)x_2]^2. \tag{22}$$

The eigenvalue problem of $\mathbf{J}$ yields a quartic characteristic equation of the form

$$\Omega^4 + p_1 \Omega^3 + p_2 \Omega^2 + p_3 \Omega + p_4 = 0, \tag{23}$$

where

$$p_1 = -(a_3 + b_4), \qquad p_2 = a_3 b_4 - b_3 a_4 - d_2 - c_1,$$

$$p_3 = d_2 a_3 - c_2 b_3 + c_1 b_4 - d_1 a_4, \qquad p_4 = c_1 d_2 - d_1 c_2. \tag{24}$$

At the zero equilibrium, $c_i = a_i$ and $d_i = b_i$ ($i = 1, 2$), and the Jacobi matrix is equal to $\mathbf{A}$. One needs to examine the two possible critical cases: $\mathbf{A}$ has a single zero eigenvalue, which corresponds to a static bifurcation (divergence), and has a pair of pure imaginary eigenvalues, which corresponds to a Hopf bifurcation (flutter). For a single zero eigenvalue the condition is given clearly by

$$p_4 = a_1 b_2 - b_1 a_2 = 0. \tag{25}$$

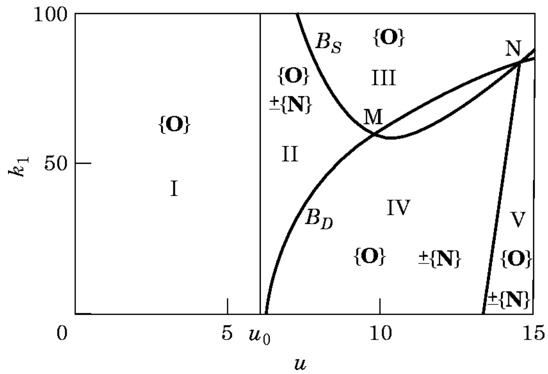

Figure 4. Sketch of stability regions.

For a purely imaginary pair the condition can be shown to be

$$p_1 p_2 p_3 - p_3^2 = p_2^2 p_4, \qquad p_3 > 0 \tag{26}$$

The stability boundaries on the $(u - k_1)$ plane derived from equations (25) and (26) are shown in Figure 4. Figures 5 and 6 show eigenvalue evolutions as u is varied in two specific cases: $k_1 = 20$ and 90, respectively. In the following analysis the nature of equilibrium is indicated by noting the signs of the real parts of the corresponding eigenvalues. Figures 4–6 show that the equilibrium is a sink in regions I and II since all the eigenvalues have negative real parts, i.e., $\Omega = (-, -, -, -)$, a saddle in region III with eigenvalues $\Omega = (+, -, -, -)$ and a saddle in regions IV and V with $\Omega = (+, +, -, -)$. In fact, crossing the boundary B_S ($\Omega = (0, -, -, -)$) from region II to III, a subcritical pitchfork bifurcation occurs; whereas by crossing B_D ($\Omega = 0, 0, -, -)$) from region II to IV, $\{\mathbf{0}\}$ undergoes a supercritical Hopf bifurcation.

The physical implication of these results is as follows. When u is relatively small, i.e., the parameters (u, k_1) lie in region I or II, the pipe is stable. For a relatively large k_1 the pipe becomes unstable (divergence) when u crosses the boundary B_S from the left, and it loses stability by flutter when u crosses B_D from the left with a relatively small k_1. These results are in agreement with the results obtained in reference [9] for a similar system without the motion-limiting constraints.

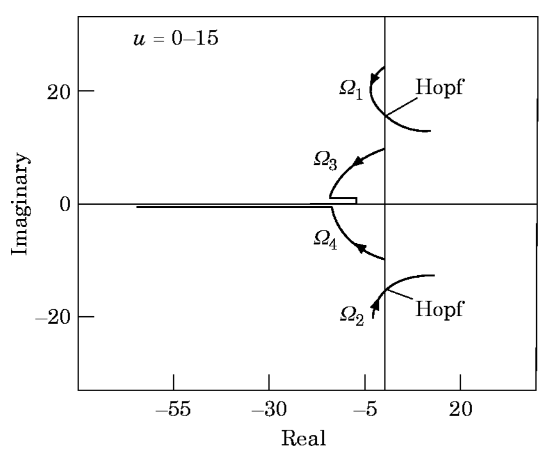

Figure 5. Eigenvalue evolutions for $\{\mathbf{0}\}$: $k_1 = 20$.

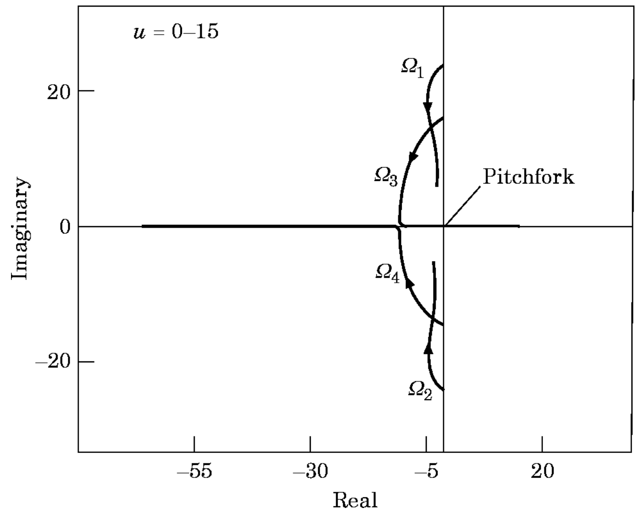

Figure 6. Eigenvalue evolutions for $\{\mathbf{0}\}$: $k_1 = 90$.

At the non-zero equilibria $\pm\{\mathbf{N}\}$, the elements of Jacobi matrix become

$$c_1 = a_1 - g_{11} I_0, \qquad c_2 = a_2 - g_{12} I_0, \qquad c_3 = a_3, \qquad c_4 = a_4,$$

$$d_1 = b_1 - g_{21} I_0, \qquad d_2 = b_2 - g_{22} I_0, \qquad d_3 = b_3, \qquad d_4 = b_4, \tag{21}$$

where

$$I_0 = 3(a_1, k + a_2)/(kg_{11} + g_{12}).$$

Eigenvalue analysis for $\mathbf{J}$ shows that the non-zero equilibria are always saddles with $\Omega = (+, -, -, -)$ in all the cases where they exist and so are always unstable. Figures 7 and 8 show eigenvalue evolutions in two specific cases: $k_1 = 20$ and 90, respectively. According to these results the bifurcation diagrams may be sketched as shown in

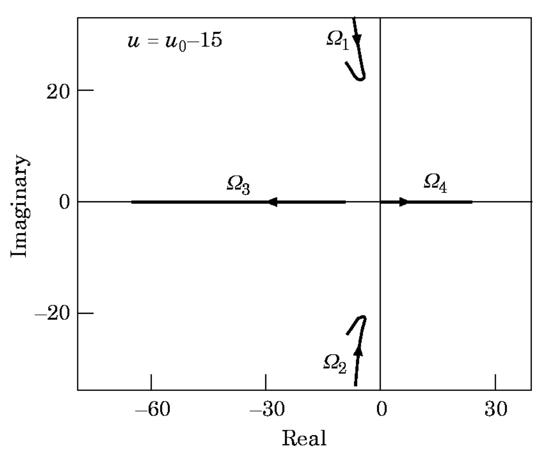

Figure 7. Eigenvalue evolutions for $\pm\{\mathbf{N}\}$: $k_1 = 20$.

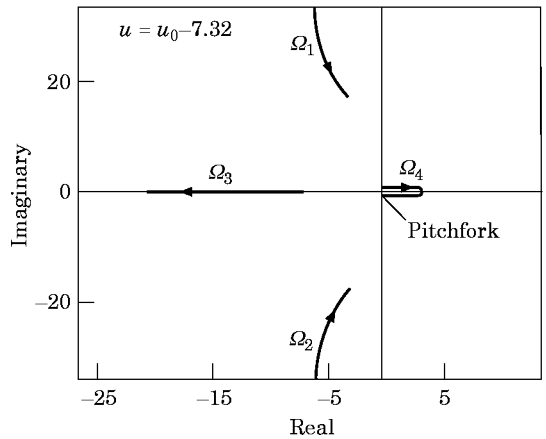

Figure 8. Eigenvalue evolutions for $\pm\{\mathbf{N}\}$: $k_1 = 90$.

Figures 9(a) and 9(b), which correspond to the cases of $k_1 = 20$ and 90, respectively. In these Figures **X** denotes the state space, and the graphs of the equilibria or closed orbits in the state space are plotted against the parameter u.

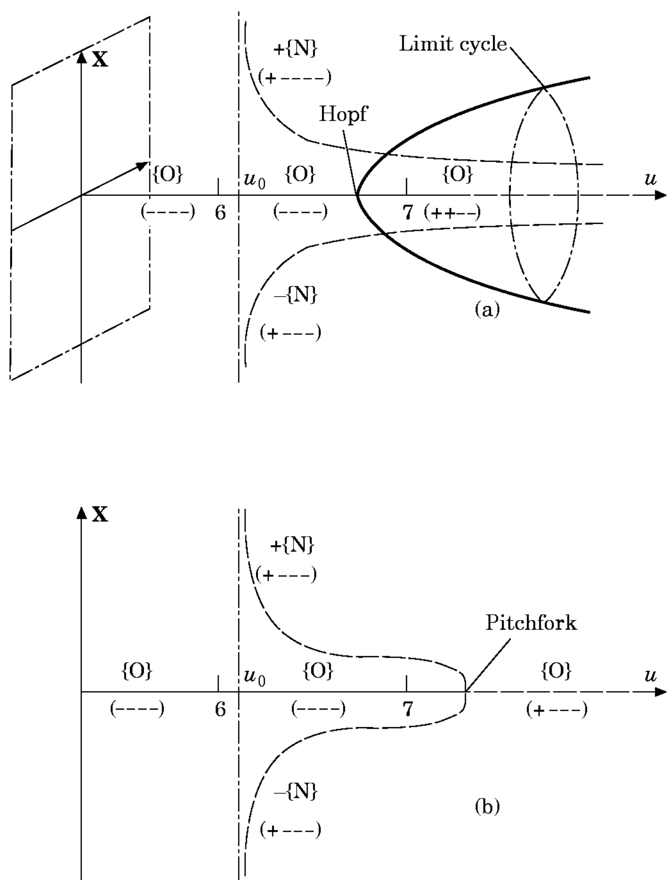

Figure 9. Bifurcation diagrams. (a) $k_1 = 20$; (b) $k_1 = 90$.

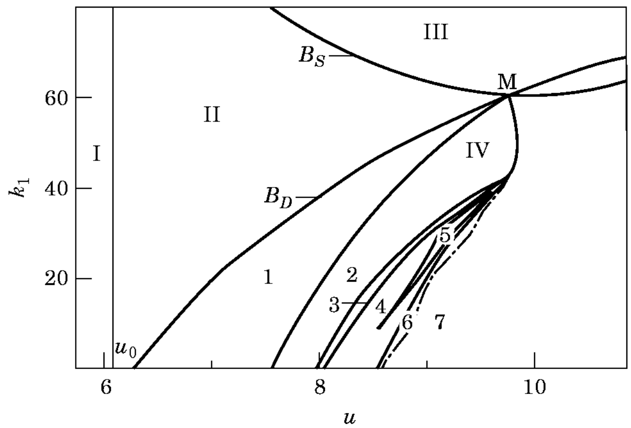

Figure 10. The "flutter region". The region is divided into seven sub regions according to different behaviour.

5. NUMERICAL ANALYSIS

In this section, it is of interest to investigate, in detail, what behaviour would occur when the parameter values lie in the "flutter region" (region IV) of Figure 4 which was determined in the previous section by local stability and bifurcation theory. In general, the theory only enables to predict the behaviour of the system for the parameter values near a point on the stability boundary, that is, the theory cannot be applied directly to the prediction of post-bifurcational behaviour when the parameter values are far from the boundary value. For this reason, the method of numerical analysis will be used here to determine the possible motions of the pipe in that region. The "flutter region" in the (u, k_1) plane was divided into a network with certain steps of u and k_1, and then numerical simulations were carried out by solving equation (5) directly with the aid of the fourth order Runge–Kutta method at every net point. The solution trajectory obtained will be projected from the four-dimensional space, (x_1, x_2, x_3, x_4) to a two-dimensional one, (x_1, x_3), and then the behaviour of the system at the net points will be determined through observation of these phase trajectories. Summarising the resuls obtained, one can divide approximately the "flutter region" into seven sub regions according to the different behaviour of the pipe, as shown in Figure 10. In region 1, the pipe undergoes limit cycle motion (flutter) with a period, the trajectory of which is symmetric. As u increases, a pitchfork bifurcation of the period solution occurs, and an asymmetric limit cycle motion arises in region 2. As u increases further, a sequence of period doubling bifurcations arises in region 3, and as a consequence of these bifurcations, chaotic motions occur in region 4. There is a period-3 window, region 5, in the range of the chaotic motions, like the phenomenon which occurs in the system with a quadratic map [10]. In region 6, the motions are chaos-like for a time, but eventually become a divergent motion, and, here, this transient chaos [11] is termed chaotic divergence. The motion in region 7 is a quick divergent motion. There are no clear-cut bounds between the regions 6 and 7. The reason why one distinguishes approximately these two regions here is merely to give rise to attention to these phenomena. Figures 11(a)–(i) show the phase portraits simulated directly from equation (7) in some specific cases, which correspond to the behaviour in regions 1–7 of Figure 10, respectively. The corresponding relation between the phase portraits in Figure 11 and the sub regions in Figure 10 is given in Table 1.

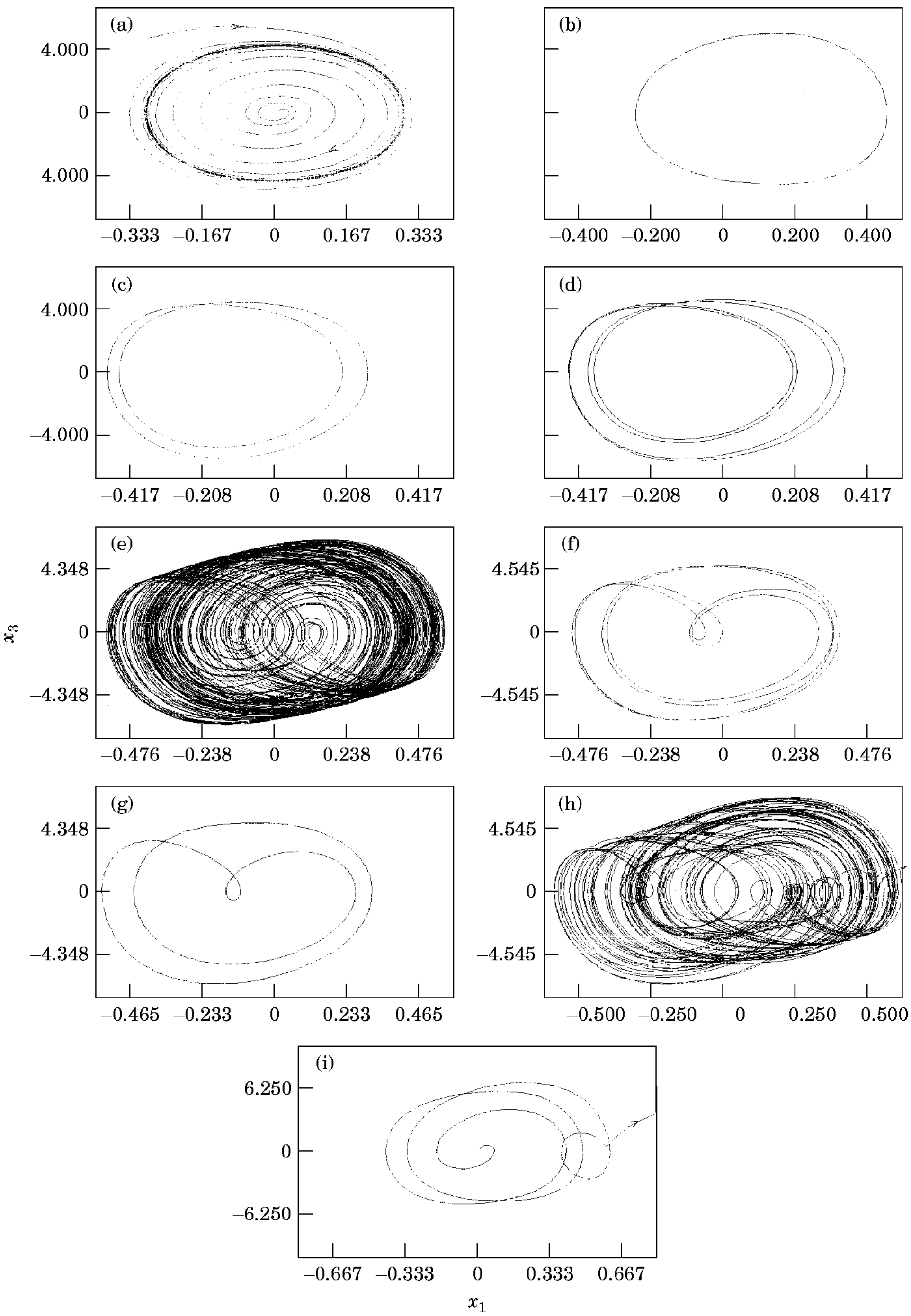

Figure 11. Numerical simulations of equation (7) projected onto (χ_1, χ_3)-plane for $k_1 = 20$, $k_2 = 100$. (a) $u = 7{\cdot}8$, symmetric limit cycle motion; (b) $u = 8{\cdot}4$. asymmetric limit cycle motion; (c) $u = 8{\cdot}75$, period-2 motion; (d) $u = 8{\cdot}58$, period-4 motion; (e) $u = 8{\cdot}75$, chaotic motion; (f) $u = 8{\cdot}81$, period-6 motion; (g) $u = 8{\cdot}83$, period-3 motion; (h) $u = 8{\cdot}99$, chaotic divergence; (i) $u = 9{\cdot}03$, divergent motion.

TABLE 1

Phase portrait relationships between Figures 11 *and* 10

Figure 11	(a)	(b)	(c, d)	(e)	(f, g)	(h)	(i)
Subregion in Figure 10	1	2	3	4	5	6	7

6. CONCLUSIONS AND DISCUSSIONS

In this paper the dynamics of a cantilevered pipe conveying fluid with the motion-limiting constraints and a spring support has been analyzed. The results obtained (Figure 4) show that for small flow velocities the trivial equilibrium (i.e., the undeformed configuration of the pipe) is always stable for any values of k_1. But, when u is relatively large, the pipe loses its stability either by divergence if k_1 is relatively large, or by flutter if k_1 is relatively small. Seven sub regions were found in the "flutter region" by using the method of numerical analysis, in each of which a different behaviour arises including the chaotic motions of the pipe. This result shows that chaotic motions can also occur in this motion-constrained pipe system with the elastic support. However, it can be seen from Figure 10 that the possibility of chaos happening becomes very small as k_1 increases. Since all the non-zero equilibria are always saddle shaped, there is no stable buckling state of the pipe in the present mathematical model, and so it would not seem that the type of chaos is one which arises through interaction between limit cycle and two sinks [2].

Note that there are two intersection points, M and N, on the boundary curve of static and dynamic instability (Figure 4). The zero equilibrium is doubly degenerate at these points. At M, the matrix **A** has a zero eigenvalue and a pair of pure imaginary eigenvalues, which corresponds to the coupled flutter and divergence bifurcation of the motion [12]; at N, another degeneracy occur: **A** has double zero eigenvalues [13]. Unfolding these codimension two bifurcation problems near the degeneracy, especially at M, the structure of phase paths in the state space around the zero and non-zero equilibria may be determined in detail, and then some information about local behaviour of the solutions in the flutter region, as well as about the chaotic motions, may be obtained. A detailed analysis on this topic will be published elsewhere.

ACKNOWLEDGMENTS

This research was supported by National Natural Science Foundation of China. The author would like to thank Ms. Y. Lin and Mr. G.-S. Zou for their assistance in numerical calculations.

REFERENCES

1. M. P. PAÏDOUSSIS 1987 *Applied Mechanics* **40**, 163–175. Flow-induced instability of cylindrical structures.
2. D. M. TANG and E. H. DOWELL 1988 *Journal of Fluids and Structures* **2**, 263–283. Chaotic oscillations of a cantilevered pipe conveying fluid.
3. M. P. PAÏDOUSSIS and F. C. MOON 1988 *Journal of Fluids and Structures* **3**, 567–591. Non-linear and chaotic fluidelastic vibrations of a flexible pipe conveying fluid.
4. M. P. PAÏDOUSSIS, G. X. LI and F. C. MOON 1989 *Journal of Sound and Vibration* **135**, 1–19. Chaotic oscillations of the autonomous system of a constrained pipe conveying fluid.

5. M. P. Païdoussis, G. X. Li and R. H. Rand 1991 *Journal of Applied Mechanics* **58**, 559–565. Chaotic motions of a constrained pipe conveying fluid: comparison between simulation, analysis, and experiment.
6. M. P. Païdoussis, T, P. Cusumand and G. S. Copeland 1992 *Journal of Applied Mechanics* **59**, 196–205. Low-dimensional chaos in a flexible tube conveying fluid.
7. G. X. Li and M. P. Païdoussis 1994 *International Journal of Non-linear Mechanics* **29**, 83–107. Stability, double degeneracy and chaos in cantilevered pipe conveying fluid.
8. M. P. Païdoussis and N. T. Issid 1974 *Journal of Sound and Vibration* **33**, 267–294. Dynamic stability of pipes conveying fluid.
9. Y. Sugiyama, Y. Tanaka, T. Kishi and H. Kawagoe 1985 *Journal of Sound and Vibration* **100**, 257–270. Effect of a spring support on the stability of pipes conveying fluid.
10. R. M. May 1976 *Nature* **261**, 459–467. Simple mathematical model with very complicated dynamics.
11. F. C. Moon 1987 *Chaotic Vibrations*. New York: John Wiley.
12. J.-D. Jin and Y. Matsuzaki 1992 *Journal of Sound and Vibration* **154**, 191–204. Bifurcation analysis of double pendulum with follower force.
13. J.-D. Jin and Y. Matsuzaki 1988 *Journal of Sound and Vibration* **126**, 265–277. Bifurcations in a two-degree-of-freedom elastic system with follower forces.